

AREAMAP AND GABOR FILTER BASED VICKERS HARDNESS INDENTATION MEASUREMENT

Andreas Maier and Andreas Uhl

Multimedia Signal Processing and Security Lab (WaveLab)
Department of Computer Sciences, University of Salzburg
J.-Haringerstr.2, 5020 Salzburg, AUSTRIA
andreas.uhl@sbg.ac.at

ABSTRACT

The automated measurement of Vickers hardness indentations is demanded from industry and is an interesting image processing challenge. Different algorithms already exist but to get reliable results for all Vickers indentation images is difficult to achieve due to large variance in indentation size, position and orientation as well as in specimen surface texture and illumination conditions. A new algorithm is presented in this paper which uses AreaMaps, the LogPolar space and Gabor filter cascades to perform indentation localisation and measurement. The new approach exhibits excellent indentation detection capabilities while at the same time providing highly accurate measurement results.

Index Terms— Vickers, hardness testing, AreaMaps

1. INTRODUCTION

The Vickers hardness test is a non-destructive material test which obtains the hardness of a workpiece by measuring the indentation caused from forcing a pyramidal indenter into the surface of the workpiece. The size of the indentation is in the sub-millimetre range thus it is inspected using a microscope with high magnification. According to international standards [1] the measurement process is carried out by determining the lengths of the diagonals of the approximately square shaped indentation and calculating the Vickers hardness value from the average of the diagonals and the applied force. A manual read out of the diagonal lengths from the indentation vertex positions is time consuming and the quality of the results depends on the operators' physical conditions like fatigue or tiredness [2].

Modern hardness testing machinery is equipped with a high resolution digital camera and an embedded computing system which allows the automation of the indentation measurement process. From the computer vision point of view, the challenge here is to produce high accurate results while the indentation images show a great variation in background and indentation texture, brightness and contrast conditions, indentation size, orientation, position and shape. See Fig. 1 for some example Vickers indentation images where the first image is a distinguished one while the others suffer from surface damages, poor optical conditions or orientation and position flaws.

Early algorithms for automated indentation measurement rely on brightness or gradient information for indentation identification.

This work has been partially supported by the Austrian Federal Ministry for Transport, Innovation and Technology (FFG Bridge 2 project no. 822682).

Images are binarised using thresholding based on pixel intensity histogram [3–5] as well as on minimised entropy [2] or the edges of indentations are computed from local gradients using a Sobel operator [6, 7] as well as by other means [8, 9]. Axes projection [3, 8, 9] supports the identification process while morphological closing [4, 5] corrects flaws that exist in the surface.

Indentation vertices are simply selected from extremal points of the segmented indentation [2, 4, 10] or are taken from the intersection of indentation edges. The accuracy of straight line edge approximation [3] is low but can be increased if done in Hough space [6, 7]. Repeating edge approximation near estimated vertices [5–7, 9, 11–13] further improves results just as corner scanning [3] or the matching of vertex templates [14, 15].

Modern algorithms use multi-resolution approaches to increase robustness and speed of the vertex detection process [11, 13, 14, 16]. These algorithms either apply template matching for indentation detection, edge approximation and vertex determination [14] or use shape prior gradient descent and level set active contour methods for the segmentation [11, 13, 16]. The use of unfocused images shows a positive influence on the indentation localisation process whether these images are used directly [12] or a shape from focus approach is used to recreate the indentation first [16].

The major problem of the above mentioned algorithms is that they perform well only on a subset of indentation images while real world indentation imagery shows a wide range of image properties which are problematic for those algorithms. Especially early algorithms are susceptible to indentation images with strong specimen surface texture or dominant artifacts. The indentation recognition rate as well as the vertex measurement accuracy are much increased in modern algorithms, expanding the range of processable indentation images but there are still many scenarios where problematic or unprocessable images occur.

In this paper a novel algorithm is presented that is completely different from known automated hardness measurement algorithms and which shows superior indentation localisation capabilities together with a very high measurement accuracy. The algorithm is described in Sec. 2, while Sec. 3 shows experiments and results achieved, which are compared to current best performing approaches. Sec. 4 concludes the paper.

2. THE ALG ALGORITHM

The measurement process for Vickers indentations relies on an exact determination of the length of the two diagonals from the indentation image. These diagonals are computed from the positions of the corresponding vertices which themselves have to be identified accu-

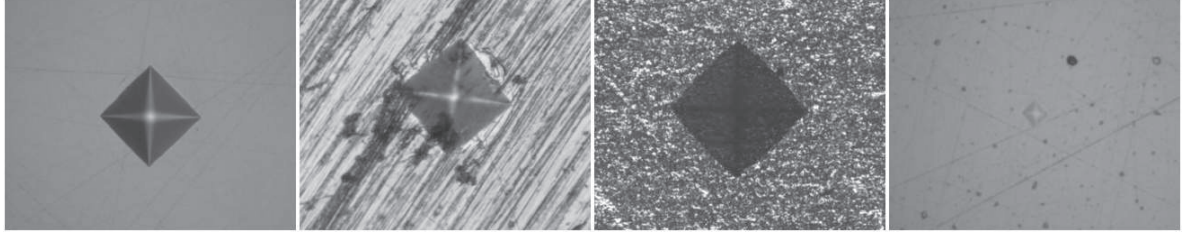


Fig. 1. Vickers indentation example images.

rately. From an image processing point of view the vertex positions are the result of the indentation detection process which can be split into a number of individual tasks (see Fig. 2).

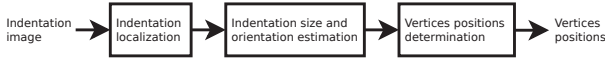


Fig. 2. Indentation detection details for automatic indentation measurement.

The proposed algorithm handles each of these individual tasks of the indentation detection chain using different technologies. The robust localisation of the indentation in the images is performed using the AreaMap operator [17], the approximation of the size and orientation of the indentation relies on template matching in the log-polar space and the determination of the vertex positions is based on Gabor filter cascades. Because of its ingredients the proposed algorithm will be called ALG algorithm (Area-map, Log-polar, Gabor).

Indentation localisation: Specific forms of the AreaMap operator (see Maier and Uhl [17]) are used to reliably localise the Vickers indentation in an indentation image. The AreaMap operator $\mathcal{A} : I \rightarrow T$ is a pixel-wise counting operator which transforms an input image I into its area map representation $T := \mathcal{A}(I)$. It is defined as

$$\mathcal{A} := T(m) = \sum_{p \in I} \chi(I, m, p) \quad \forall m \in I \quad (1)$$

where m and p are pixel coordinates and $\chi(I, m, p)$ is an indicator function. The operator therefore counts the number of pixel positions p that fulfil the constraints of the indicator function χ relative to the pixel of interest m . For the application of indentation localisation two different indicator functions are used:

$$\chi_{DecAMap}(I, m, p) := \begin{cases} 1, & \text{if } ngb(p, p') \text{ and } I(p) \leq I(p') \\ & \text{and } \chi_{DecAMap}(I, m, p') = 1, \\ 0, & \text{otherwise} \end{cases} \quad (2)$$

and

$$\chi_{IncAMap}(I, m, p) := \begin{cases} 1, & \text{if } ngb(p, p') \text{ and } I(p) \geq I(p') \\ & \text{and } \chi_{IncAMap}(I, m, p') = 1, \\ 0, & \text{otherwise} \end{cases} \quad (3)$$

where $ngb(p, p')$ indicates that pixel p and p' are (4-)connected neighbours and $I(p)$ is the value of the pixel p in the image I . The function $\chi_{DecAMap}$ indicates the property that a pixel p is connected to the start pixel m through a sequence of pixels with decreasing values. Similarly, the function $\chi_{IncAMap}$ indicates a sequence of increasing pixel values on a arbitrary path from m to p . Following

the considerations outlined in [17] it is not necessary to calculate the full DecAMap and IncAMap but sparse versions are enough for the intended purpose. From the AreaMaps the indentation centre has to be computed following the procedure described in the section ‘‘Indentation centre determination’’ in [17].

Size and orientation approximation: The log-polar transform turns out to be a helpful tool for estimating the dimensions of the indentation in a robust and fast way. It is defined as

$$(x_r, y_r) \rightarrow (\rho, \theta) := \begin{cases} \rho = \log \sqrt{x_r^2 + y_r^2} \\ \theta = \arctan x_r/y_r \end{cases} \quad (4)$$

where (x_r, y_r) are Cartesian coordinates relative to an origin (x_o, y_o) and (ρ, θ) are the corresponding log-polar transformations. If the origin is located at the centre of an indentation then the log-polar space representation of that indentation shows two interesting properties: (i) The transformed indentation always has the same shape, independent of the original indentation size. The size just defines the offset of the horizontal position of the edge lines. (ii) A rotation of the original indentation is transformed into a vertical offset of the log-polar representation. See Fig. 3 for two indentation images and their log-polar transforms, respectively. The log-polar transform is thereby partially extended in the vertical direction to simplify subsequent processing.

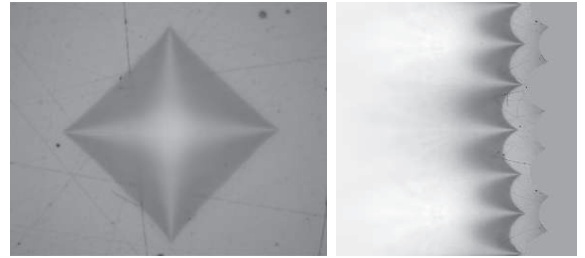


Fig. 3. Example of indentation image and its log-polar representations.

The properties of the indentation in the log-polar space representation can be exploited to identify indentation edges and their orientations. Using a single template and template matching, for example normalised cross-correlation, identifies all four edges simultaneously. This is done in a very robust manner as artifacts that are often found outside of the indentation are given decreased weight due to the log-polar transform. Fig. 4 shows an example of the edge template and the result of the template matching. The match exhibits four distinct maxima at the positions of the edges. These maxima are horizontally aligned and equally spaced in the vertical direction,

therefore a fixed filter can be used to detect them. The applied filter operation is actually another normalised cross-correlation of the filter with the match. Back-projecting the positions of the filtered maxima into the original image identifies the midpoints of the indentation edges while back-projecting to the log-polar space gives the rotation of the indentation.

The fixed filter is shown as the last element of Fig. 4. It has detection regions which are lens-shaped (i.e. with elliptical support) so this filter is strict to angle errors but allows slight miss-alignment of the edges relative to the indentation centre. (This happens if the estimated centre was somewhat displaced initially, see Fig 3.)

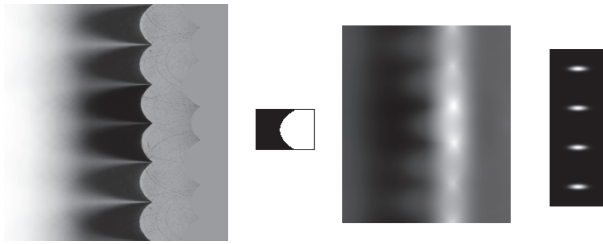


Fig. 4. Example log-polar image, edge template, matching result and edge position filter.

For the majority of the indentation images the indentation localisation process identifies a point that is close to the indentation centre and a good origin for the log-polar transform. However, for a few images the identified point is further away from the indentation centre and the proposed size estimation will fail. This case is detectable and can be corrected. If any of the maxima identified from the filter in the match is less than 50% of the best value than such a centre location error is presumed and an iterative re-centring procedure takes place. For re-centring, the horizontal lines of failed maxima are searched for individual best values and these positions are taken as the correct edge locations instead of the proposed positions. The centre estimate from indentation localisation is corrected using the new edge positions. The size and orientation approximation step is repeated with the new centre estimate until the centre position stabilises after a few iterations. Fig. 5 shows the effect of an incorrect indentation centre estimate.

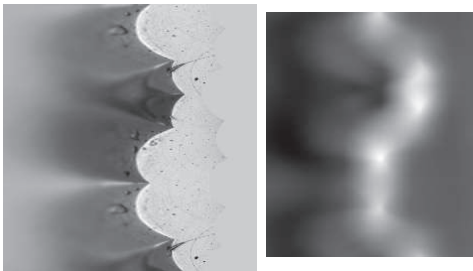


Fig. 5. Example of a log-polar transform with corresponding match from a misplaced origin.

Determination of the vertex positions: Regular indentation images, especially if taken with a high resolution imaging system, show degraded and fringed indentation edges and vertices. The reason for this is on one hand that the optical system introduces significant blur at high magnifications and on the other hand that the

surface of workpieces is textured, scratched, rusty, dirty and full of holes, grooves and artifacts. Furthermore, edges are not straight lines but can be convex or concave to a certain extend. It is therefore difficult to identify vertices either directly or to accurately construct edge contours that can be intersected to get the vertex positions.

The approach taken for the algorithm in this paper is to do a coarse-to-fine approximation of the edges near the vertices using cascading Gabor filters. A Gabor filter is computed as

$$g(x, y; \lambda, \theta, \psi, \sigma, \gamma) = e^{-(x'^2 + \gamma^2 y'^2)/2\sigma^2} \sin(2\pi \frac{x'}{\lambda} + \psi) \quad (5)$$

with

$$x' = x \cos \theta + y \sin \theta \quad y' = -x \sin \theta + y \cos \theta$$

where θ represents the orientation of the filter, σ and γ are the parameters for the Gaussian envelope and its aspect ratio, λ and ψ are the wavelength and phase offset of the sinusoidal factor.

The Gabor filters are used in the proximity of vertices to approximate the adjacent edges. For that reason a filter is split into two halves from which only one half is applied to a respective edge while the other half is ignored. The origin of the filter is placed at the estimated vertex position and allowed to move perpendicular to the direction of the edge in a limited range to improve the filter response. The best filter response is taken as the new vertex position which itself serves as the vertex estimate for the next iteration. The next iteration starts after both adjacent edges have been processed. It uses scaled down Gabor filters and limits the range in which the filters are applied. The initial estimate of the vertex positions is calculated from the indentation approximation of the previous step and the iteration stops when the filter arrives at its minimal size. See Fig. 6 for a schematic presentation of the principle.

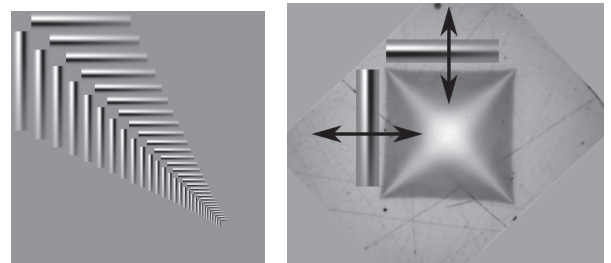


Fig. 6. Gabor half-filter cascades and principle of operation for the upper left vertex.

For the intended application the following parameters show the best results: the spacial aspect ratio of the Gaussian envelope $\gamma = 0.1$, the initial half-filter height h is equal to the edge length, the filter scale down is 10% for each iteration, the iteration stops at the minimum height $h = 12$ pixel, $\psi = 0$, λ is equal to the filter width w and $\sigma = 0.3(h/2 - 1) + 0.8$. The filter orientation depends on the orientation ϕ of the indentation and will have the values $\theta = \{\phi, \phi + \pi/2, \phi + \pi, \phi + 3\pi/2\}$ corresponding to the angles of the edges. To better handle convex indentations additional filter orientations are considered as long as the filter height is at least half of the edge length and bigger than 100 pixel. In this case the filter is also positioned and evaluated at angles of 0.05 and 0.1 rad relative to the corresponding edges. The filter operation itself is implemented as a cross-correlation of the filter with an image region.

3. EXPERIMENTS

The proposed ALG algorithm has been evaluated against selected Vickers indentation images which are difficult to measure with known automated algorithms. The optical system of the employed emcoTEST DuraScan hardness testing equipment is composed of a microscope with a magnification of 10x–100x and a digital camera with a resolution of 1280x1024 pixel at 8 bit gray scale. The ALG results are compared to the results achieved with two current state-of-the-art algorithms, the “3-Stage Multi-Resolution Template-Matching (3SMRTM)” approach [14] and the “Shape-Prior Active Contours (SPAC)” approach [11]. The coding scheme for all example images in this section is chosen such that vertices identified by ALG are marked with a single cross (violet colour), by 3SMRTM with a cross in a circle (orange colour) and by SPAC with a cross in a square (blue colour).

The first property to demonstrate for the ALG algorithm is the enhanced indentation identification capability. Fig. 7 shows examples of indentation images for which the indentation localisation fails for one or more of the examined algorithms. The markers are strongly amplified to make them clearly visible in the figure.

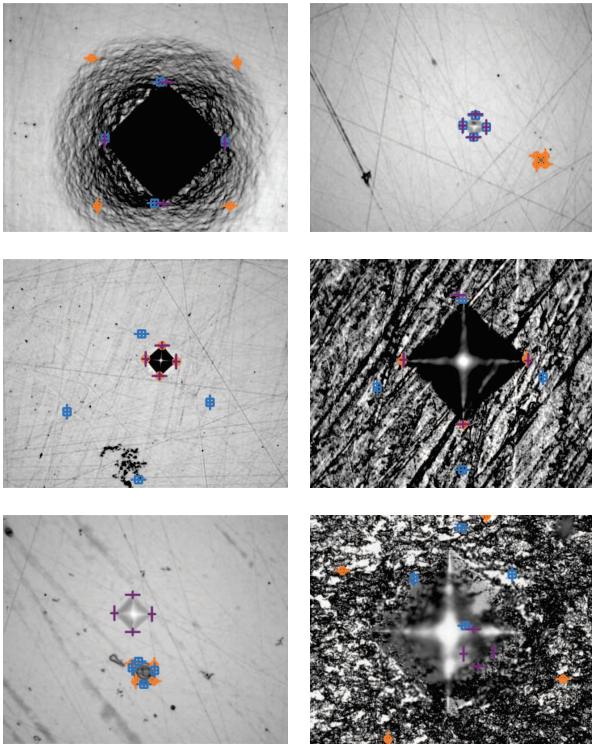


Fig. 7. Selected results achieved with ALG (violet single cross), 3SMRTM (orange cross in circle) and SPAC (blue cross in square) algorithm.

The first row demonstrates how the 3SMRTM algorithm is misled by surface artifacts. The left image has a dark accumulation of material around the indentation which has a good contrast to the surrounding and which is approximately square shaped. The accumulation presents a wrong orientation but because 3SMRTM is rotation invariant it is more attracted by the accumulation. The right image also has a very dark spot, this time from a hole in the surface,

which again attracts the 3SMRTM algorithm. The second row in the figure demonstrates failures of SPAC. The left image show that the shrinking active contour can not overcome the dominant artifact in the lower image region while the right image contains irritating gradient information that again influences the gradient descent step. All four images are well handled by ALG which is also true for the first image in the last row where both, 3SMRTM and SPAC, fail to localise the indentation because a surface artifact once again looks to attractive. The second image in the last row is an example for an indentation that is extraordinary difficult to segment thus all three regarded algorithms fail.

The second property, the high accuracy of the vertex determination, is demonstrated in Fig. 8 which shows detailed views of vertices that have been magnified for better visibility. All indentation images suffer from strong textures in the specimen surface and from difficult illumination and contrast conditions. The image contrast can be high while the contrast of the indentation itself is surprisingly low as in the very first and very last image, or the overall image contrast is low for all elements, as for the images in the middle row. The ALG algorithm shows results that are more accurate than the vertex positions determined by 3SMRTM or SPAC for the first four images. The images in the last row are difficult to handle correctly for all three algorithms but the magnitude of the error is somehow similar. To ultimately determine the correct vertex location for the cases in the example images is a likewise difficult task for a human too and may often be impossible without the inclusion of a bigger image regions.

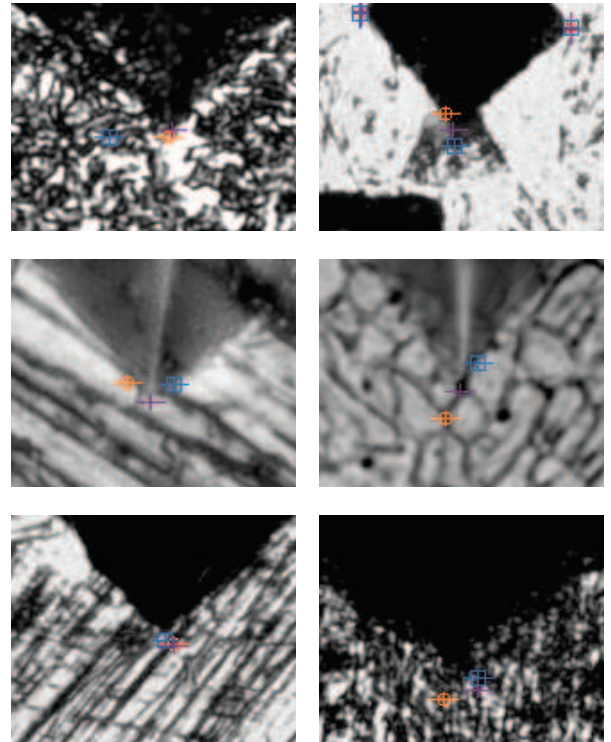


Fig. 8. Selected vertex details achieved with ALG (violet single cross), 3SMRTM (orange cross in circle) and SPAC (blue cross in square) algorithm.

The ALG algorithm has been further evaluated on the Vickers

indentation image databases described in [14]. The databases are complemented by ground truth of vertex positions measured by hardness testing experts. The achieved results are slightly better than the results of 3SMRTM [14] and SPAC [11] in the accuracy of vertex positions and the number of outliers. This behaviour is expected since the databases include a considerable number of less critical indentation images for which the other algorithms yield good measurements too, so that their results are already very accurate. In this case the ALG algorithm mainly stands out for the problematic indentation images which adds up to the observed improvements.

The average runtime per image of the discussed ALG approach is 3.6 seconds. All code is implemented in Python with the help of the OpenCV library and executed on a laptop computer (1.6GHz Pentium-M, 512MB RAM). An implementation in C or a similar language is expected to provide additional speed-up. The achieved speed is higher than manual measurements and is close to interactive performance.

4. CONCLUSION

The novel ALG algorithm proposed in this paper shows distinguished results in the measurement of Vickers hardness indentation images. On one hand it has a very robust and reliable indentation localisation while on the other hand it demonstrates high accuracy in the determination of vertex positions. Both propositions have been verified against the currently best performing algorithms 3SMRTM and SPAC. The speed of the ALG algorithm is high and competitive to manual measurement. The ALG algorithm should be adaptable to other hardness tests like Knoop or Brinell as well through small modifications of the shape of the Gabor filters.

5. REFERENCES

- [1] ASTM Standard E384, (2010e2), "Standard test method for Knoop and Vickers hardness of materials," in *ASTM Standards*. 2010, ASTM International, West Conshohocken, PA, DOI: 10.1520/E0384-10E02, www.astm.org.
- [2] P. P. R. Filho, T. S. Cavalcante, V. H. de Albuquerque, and Joao M. R. S. Tavares, "Brinell and Vickers hardness measurement using image processing and analysis techniques," *Journal of Testing and Evaluation*, vol. 38, no. 1, pp. JTE102220, 2010.
- [3] Takao Sugimoto and Tadao Kawaguchi, "Development of an automatic Vickers hardness testing system using image processing technology," *IEEE Transactions on Industrial Electronics*, vol. 44, no. 5, pp. 696–702, Oct. 1997.
- [4] Vilson Mendes and Fabiana Leta, "Automatic measurement of Brinell and Vickers hardness using computer vision techniques," in *Proceedings of the XVII IMEKO World Congress*, Dubrovnik, Croatia, June 2003, pp. 992–995.
- [5] M. Macedo, V.B. Mendes, A. Conci, and F.R. Leta, "Using hough transform as an auxiliary technique for vickers hardness measurement," in *Proceedings of the 13th International Conference on Systems, Signals and Image Processing (IWS-SIP'06)*, 2006, pp. 287–290.
- [6] Yong Pan, Yuekang Shan, Yu Ji, and Shibo Zhang, "A new method for automatically measuring vickers hardness based on region-point detection algorithm," *Proc. of the Fourth International Symposium on Precision Mechanical Measurements*, vol. SPIE 7130, pp. 71304C–71304C–6, 2008.
- [7] Y. Ji and A. Xu, "A new method for automatically measurement of vickers hardness using thick line hough transform and least square method," in *Proceedings of the 2nd International Congress on Image and Signal Processing (CISP'09)*, 2009, pp. 1–4.
- [8] Leehter Yao and Chih-Heng Fang, "An automatic hardness measuring method using hough transform and fuzzy c-means algorithm," in *Fuzzy Systems, 2001. The 10th IEEE International Conference on*, dec. 2001, vol. 2, pp. 842 – 847 vol.3.
- [9] L. Yao and C.-H. Fang, "A hardness measuring method based on hough fuzzy vertex detection algorithm," *IEEE Trans. on Industrial Electronics*, vol. 53, no. 3, pp. 963–973, 2006.
- [10] Wang Guitang, Zhu Jianlin, and Cao Peiliang, "Application of fractal dimension and co-occurrence matrices algorithm in material vickers hardness image segmentation," in *Proceedings of the 3rd international conference on Intelligent information technology application*, Piscataway, NJ, USA, nov. 2009, vol. 3 of *IITA'09*, pp. 624–627, IEEE Press.
- [11] Michael Gadermayr and Andreas Uhl, "Dual-resolution active contours segmentation of Vickers indentation images with shape prior initialisation," in *Proceedings of the 5th International Conference on Image and Signal Processing (ICISP'12)*, A. Elmoataz, D. Mammass, O. Lezoray, F. Nouboud, and D. Aboutajdine, Eds., Agadir, Morocco, June 2012, vol. 7340 of *Springer LNCS*, pp. 362–369.
- [12] Michael Gadermayr, Andreas Maier, and Andreas Uhl, "The impact of unfocused Vickers indentation images on the segmentation performance," in *Proceedings of the 8th International Symposium on Visual Computing (ISVC'12)*, George et al Bebis, Ed., Rethymno, Greece, July 2012, vol. 7432 of *Springer LNCS*, pp. 368–378.
- [13] M. Gadermayr, A. Maier, and A. Uhl, "Active contours methods with respect to vickers indentations," *Machine Vision and Applications*, pp. 1–14, 2012.
- [14] M. Gadermayr, A. Maier, and A. Uhl, "Robust algorithm for automated microindentation measurement in Vickers hardness testing," *Journal of Electronic Imaging*, vol. 21, pp. 021109, 2012.
- [15] M. Gadermayr, A. Maier, and A. Uhl, "Algorithms for microindentation measurement in automated Vickers hardness testing," in *Tenth International Conference on Quality Control for Artificial Vision (QCAV'11)*, J.-C. Pinoli, J. Debayle, Y. Gavet, F. Cruy, and C. Lambert, Eds., St. Etienne, France, June 2011, number 8000 in *Proceedings of SPIE*, pp. 80000M–1 – 80000M–10, SPIE.
- [16] Michael Gadermayr and Andreas Uhl, "Image segmentation of Vickers indentations using shape from focus," in *Proceedings of the International Conference on Image Analysis and Recognition (ICIAR'12)*, Aurilio J. C. Campilho and Mohamed S. Kamel, Eds., Aveiro, Portugal, June 2012, vol. 7324 of *Springer LNCS*, pp. 149–157.
- [17] A. Maier and A. Uhl, "The areamap operator and its application to vickers hardness testing images (invited paper)," *International Journal of Future Generation Communication and Networking (Special Issue on Image and Signal Processing Best papers of ICISP 2012)*, vol. 5, no. 4, pp. 1–16, 2012.